

Article

Three Component Controls in Pillared Metal-Organic Frameworks for Catalytic Carbon Dioxide Fixation

Jinmi Noh ¹, Dasom Kim ¹, Jihyun Lee ², Minyoung Yoon ², Myung Hwan Park ³ ,
Kang Mun Lee ^{4,*}, Youngjo Kim ^{1,*} and Min Kim ^{1,*}

¹ Department of Chemistry and BK21Plus Research Team, Chungbuk National University, Cheongju, Chungbuk 28644, Korea; njm0902@gmail.com (J.N.); 7.24dasomkim@gmail.com (D.K.)

² Department of Nanochemistry, College of Bionano, Gachon University, Sunghnam 13120, Korea; jh_christina@naver.com (J.L.); myyoon@gachon.ac.kr (M.Y.)

³ Department of Chemistry Education, Chungbuk National University, Cheongju, Chungbuk 28644, Korea; mhpark98@chungbuk.ac.kr

⁴ Department of Chemistry, Institute for Molecular Science and Fusion Technology, Kangwon National University, Chuncheon, Gangwon 24341, Korea

* Correspondence: kangmunlee@kangwon.ac.kr (K.M.L.); ykim@chungbuk.ac.kr (Y.K.); minkim@chungbuk.ac.kr (M.K.); Tel.: +82-43-261-2283 (M.K.)

Received: 25 October 2018; Accepted: 16 November 2018; Published: 20 November 2018



Abstract: Three components of pillared metal-organic frameworks (MOFs, three components = metal ion, carboxylic acid ligand, and *N*-chelating ligand) were controlled for CO₂ cycloaddition catalysts to synthesize organic cyclic carbonates. Among the divalent metals, Zn²⁺ showed the best catalytic activity, and in DABCO (1,4-diazabicyclo[2.2.2]octane)-based MOFs, hydroxy-functionalized DMOF-OH was the most efficient MOF for CO₂ cycloaddition. For the BPY (4,4'-bipyridyl)-type MOFs, all five prepared BMOFs (BPY MOFs) showed similar and good conversions for CO₂ cycloaddition. Finally, this pillared MOF could be recycled up to three times without activity and crystallinity loss.

Keywords: metal-organic framework; coordination polymer; catalysis; carbon dioxide; cycloaddition

1. Introduction

The repeating coordination bonds between metal clusters (or ions) and multi-topic ligands produce coordination polymers (CPs). When CPs have three-dimensional structures with empty pores, they are also called metal-organic frameworks (MOFs) [1,2]. In the last decade, a variety of applications for utilizing the empty pores of MOFs have been developed, such as gas separation and storage, molecular shuttling and storage, sensing, etc. [3–5]. In addition, the catalytic applications of MOFs have been intensively explored, since the pores of MOFs could allow controllable reaction sites, and each component of MOFs (metal clusters and organic ligands) could be employed as a catalytic species for organic transformations [6–10].

MOF-based chemical CO₂ fixation is one of the most widely studied organic transformations in a heterogeneous manner [11,12]. The coupling reaction between carbon dioxide and epoxide to form organic cyclic carbonates is efficient and useful CO₂ fixation, and organic cyclic carbonates are key molecules for polar organic solvents and industrial polymerization [13]. This reaction is also called the cycloaddition of CO₂ with epoxide. Various MOFs from a wide range of metal sources have been examined for the cycloaddition of CO₂ under thermal treatment, and basically, the Lewis acid site of the metal cluster in MOFs acts as a catalytic site for CO₂ and epoxide activation [11]. Recently, we have investigated the effects of organic functional groups on zirconium-based MOF (i.e., UiO-66;

UiO = University of Oslo) catalysts for CO₂ cycloaddition. Among the eight different functionalities, the hydroxy group showed the best catalytic conversion of CO₂ to organic cyclic carbonates under the high temperature condition (140 °C), and the non-functionalized UiO-66 showed good catalytic activity under the low temperature condition (50 °C) [14]. However, the control and tuning of MOFs for CO₂ cycloaddition catalyst are mainly limited on the structural effect along with metal cation's effect or the functional group effects with same metal and frameworks. To maximize the advantage of MOF-based catalysts, the fine-tuning on ligands, pillar ligands (additional ligands), and metal cations should be studied at the same time.

Herein, we have expanded our approach to three component controls in pillared MOFs for fine-tuning MOF-based catalysts for CO₂ cycloaddition. The pillared MOF consists of two different ligands and metal clusters. The metal clusters in MOFs are also called the secondary building units (SBUs). Generally, dicarboxylic acid ligands and nitrogen-donating ligands are employed together for pillared MOF synthesis. From a structural viewpoint, the SBUs and dicarboxylate ligands form the 2D sheet, and N-donor ligands connect two 2D sheets through coordination bonds between the metal on the SBU and N-atom on the ligand (Figure 1). We have examined the effects of the metal cation in the SBU, various functional groups on the benzene-1,4-dicarboxylic acid (BDC) ligand, and the pillar ligand for CO₂ cycloaddition. The best combination of a pillared MOF for efficient catalysis of chemical CO₂ fixation has been finalized.

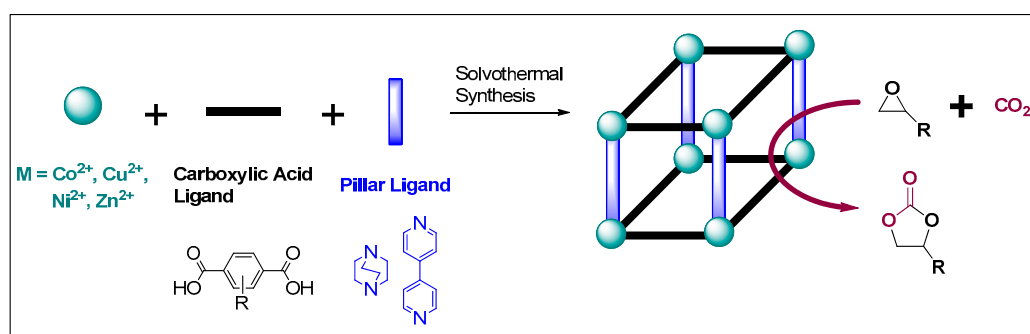


Figure 1. Three components in pillared metal-organic frameworks (MOFs) and CO₂ cycloaddition.

2. Results

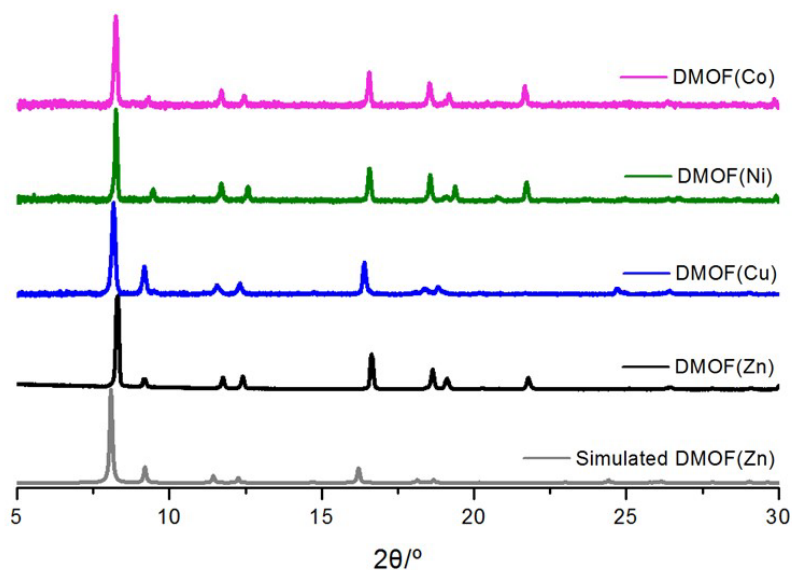
DMOF (DABCO MOF) is the representative pillared MOF, which consists of a metal cluster (i.e., SBU), benzene-1,4-dicarboxylic acid (BDC), and DABCO (i.e., 1,4-diazabicyclo[2.2.2]octane) [15,16]. The dimeric paddle-wheel-type SBU is connected with four BDC ligands in the equatorial positions and two DABCO ligands in the axial positions. Thus, the empirical formula of DMOFs is denoted as M₂(BDC)₂(DABCO). At the outset of our exploration of pillared MOFs for CO₂ cycloaddition [17], we have focused on this DMOF series, since the DABCO component is a tertiary amine and it will be a good catalyst for CO₂ cycloaddition [18].

Propylene oxide (**1a**) was employed as a model substrate to react with CO₂ (under 10 bar) in the presence of DMOF and ammonium salt co-catalysts without additional solvent (Table 1). The zinc-based DMOF (DMOF(Zn)) was used for the first trial of a MOF catalyst in this study, since DMOF(Zn) is common for functionalization with ligands. Whereas a low conversion was obtained with DMOF(Zn) alone (8%, entry 1, Table 1), the addition of a co-catalyst salt provided increased reactivity under 100 °C for 3 h. Among the five ammonium and phosphonium salts with various halides (TBAI, tetra-*n*-butylammonium iodide; TBABr, tetra-*n*-butylammonium bromide; TBACl, tetra-*n*-butylammonium chloride; TBPBr, tetra-*n*-butylphosphonium bromide; and PPNCl, bis(triphenylphosphine)iminium chloride), TBABr showed the best efficiency (entries 2–6, Table 1). Only 33% conversion was observed (entry 7, Table 1) when the co-catalyst TBABr was employed alone.

Table 1. Reaction condition screening and metal effects.

Entry	MOF Catalyst	Co-Catalyst	Time (h)	Conversion (%)
1	DMOF(Zn)	-	3	8
2	DMOF(Zn)	TBAI	3	45
3	DMOF(Zn)	TBABr	3	94
4	DMOF(Zn)	TBACl	3	71
5	DMOF(Zn)	TBPBr	3	76
6	DMOF(Zn)	PPNCl	3	60
7	-	TBABr	3	33
8	DMOF(Zn)	TBABr	2	69
9	DMOF(Co)	TBABr	2	39
10	DMOF(Ni)	TBABr	2	30
11	DMOF(Cu)	TBABr	2	19

The effect of the metal cation on CO₂ cycloaddition was examined next. A series of DMOFs with different metal salts (e.g., Co, Ni, Cu, and Zn) were prepared following the reported procedures (see the experimental section and supplementary information for details). All of the DMOFs from Co, Ni, Cu and Zn showed identical structures and matched with previously reported pillared MOF structures, as indicated by powder X-ray diffraction (PXRD) patterns (Figure 2). Under the optimized reaction conditions (100 °C, 1 mol% TBABr) with a shortened reaction time (2 h) to display reactivity differences better, DMOF(Zn) showed the best conversion (entry 8, Table 1), and the catalytic efficiency decreased according to the following sequence: DMOF(Co) > DMOF(Ni) > DMOF(Cu) (entries 9–11, Table 1), which is exactly the same trend recently reported by Verpoort's group. In their study, DMOFs from different metals were employed for CO₂ cycloaddition without co-catalysts [19].

**Figure 2.** Powder X-ray diffraction (PXRD) patterns of DMOFs with different metal sources.

With DMOF(Zn) and the optimized conditions, the effect of the functional group on the BDC ligand was studied next (Table 2). We have prepared five different DMOF(Zn)s with

different BDC ligands, such as BDC, BDC-NH₂ (2-aminobenzene-1,4-dicarboxylic acid), BDC-OH (2-hydroxybenzene-1,4-dicarboxylic acid), 1,4-NDC (naphthalene-1,4-dicarboxylic acid), and 2,6-NDC (naphthalene-2,6-dicarboxylic acid, see the supplementary information for details). DMOF(Zn), DMOF(Zn)-NH₂, DMOF(Zn)-OH, and DMOF(Zn)-1,4-NDC showed identical structures and matched well with the reported structures, which was demonstrated by PXRD (Figure 3) [20–22]. Only DMOF(Zn)-2,6-NDC showed a little different pattern, since the two dicarboxylic acids were a slightly tilted from the other BDC ligands. However, they are all still in the same framework and have the empirical formula Zn₂(BDC)₂(DABCO), as indicated by ¹H NMR (Nuclear Magnetic Resonance) after acid digestion (Figures S1–S5 in the Supplementary Information). And the crystal size was determined by microscope, since DMOFs were obtained as large single crystals. Around 0.5–2 mm size transparent crystals were synthesized from the solvothermal condition (Figure S6).

Table 2. Functional group controls in DMOF(Zn)s.

Entry	MOF Catalyst	Conversion (%)	Selectivity (%)
1	DMOF(Zn)-NH ₂	75	>99
2	DMOF(Zn)-OH	83	>99
3	DMOF(Zn)-1,4-NDC	62	>99
4	DMOF(Zn)-2,6-NDC	69	>99

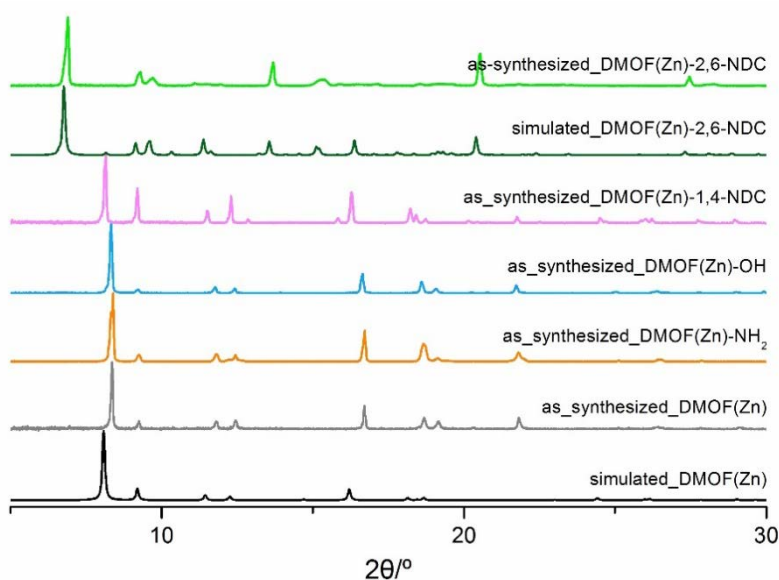


Figure 3. Powder X-ray diffraction (PXRD) patterns of DMOFs with different functionalities on the benzene-1,4-dicarboxylic acid (BDC) ligand.

Among the five DMOF(Zn)s, the hydroxy-functionalized DMOF(Zn)-OH showed the best conversion for CO₂ cycloaddition with **1a** (83%, entry 2 in Table 2). The selectivity for cyclic carbonate synthesis versus polymerization was also measured by ¹H NMR, and no polycarbonates were detected. The amino-functionalized DMOF(Zn)-NH₂ also displayed good catalytic efficiency under the optimized conditions (75%, entry 1 in Table 2). This finding is quite relevant to a previous

study on the effects of functional groups on a zirconium-based MOF for CO₂ cycloaddition. In the case of the Zr-MOF, the hydroxy-group was also the best catalyst at high temperature (140 °C) in the presence of a co-catalyst, TBAI (tetra-*n*-butylammonium iodide) [14].

For the last part of MOF catalyst tuning, we introduced a 4,4'-bipyridyl (BPY) ligand as a pillar ligand, which is longer than DABCO. This type of MOF is also known as BMOF (BPY-MOF), and it has a similar empirical formula M₂(BDC)₂(BPY) [23,24]. We fixed the metal part to be Zn and controlled the functional group on ligands with BPY pillar. A series of BMOFs, such as BMOF(Zn), BMOF(Zn)-NH₂, BMOF(Zn)-OH, BMOF(Zn)-1,4-NDC, and BMOF(Zn)-2,6-NDC, were obtained by following the reported procedures or modified methods (see the supplementary information for details). BMOF(Zn) and BMOF(Zn)-NH₂ showed identical structures, as indicated by PXRD (Figure 4), which matched well with the reported structures for BMOF(Zn)-1,4-NDC and BMOF(Zn)-2,6-NDC. The ¹H NMR after acid digestion revealed the formulas of the BMOF(Zn)s, except BMOF(Zn)-OH is Zn₂(BDC-R)₂(BPY) (Figures S7–S11 in the supplementary information). Since the particle size of BMOF(Zn)s were smaller than DMOF(Zn)s, Scanning Electron Microscope (SEM) images were obtained and analyzed for particle size. BMOF(Zn), BMOF(Zn)-NH₂, and BMOF(Zn)-1,4-NDC showed particles size with ~200 μm size, and BMOF(Zn)-2,6-NDC showed smaller particle size with ~50 μm. Lastly, BMOF(Zn)-OH has needle type crystals with ~200 μm length and ~20 μm width (Figure S12). Interestingly, there are no reported structures for BMOF(Zn)-OH in the literature, and thus we have confirmed the structure of BMOF(Zn)-OH by single X-ray crystallography (see the supplementary information for details, Tables S1 and S2) and measured gas sorption property along with thermal stability. Surprisingly, BMOF(Zn)-OH showed a different structure compared with the other BMOF(Zn)s. Four 4,4'-BPY ligands were coordinated with the Zn₂-SBU at the same time (Figure S13). Based on the structural analysis, the empirical formula of BMOF(Zn)-OH is Zn₂(BDC-OH)(BPY), and the hydroxy group, due to its role in hydrogen bonding with the Zn₂ SBU, leads to this structural change. Brunauer-Emmett-Teller (BET) surface area is calculated for 70 m²/g, which is lower porosity than reported BMOF(Zn)-2,6-NDC (Table S3). Full N₂ isotherm also performed at 77 K and displayed a hysteresis on a range between 0.4–1.0 relative pressure, as shown in Figure S14. Last, the thermal stability of BMOF(Zn)-OH was measured by thermogravimetric analysis (TGA). New material is thermal stable up to >200 °C and showed 80% weight loss at 500 °C (Figure S15).

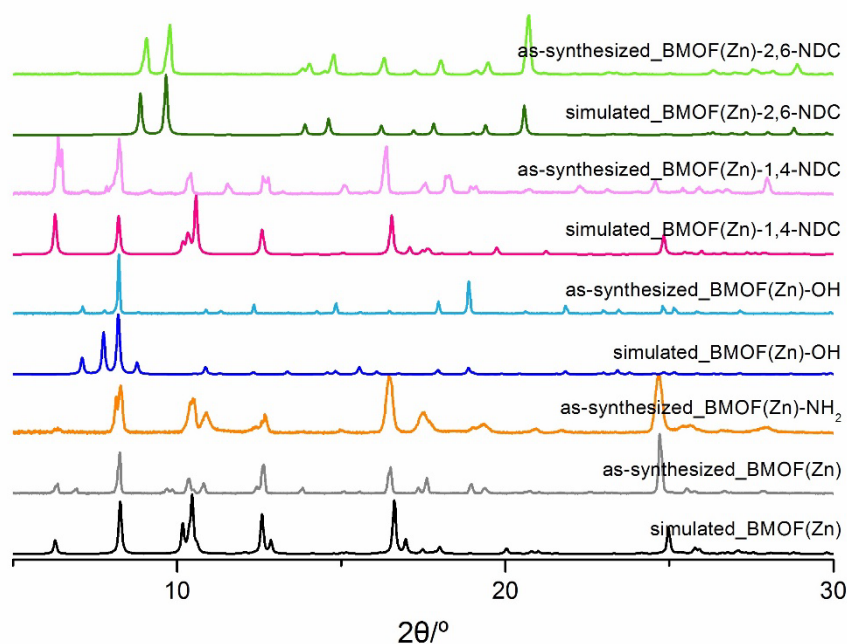
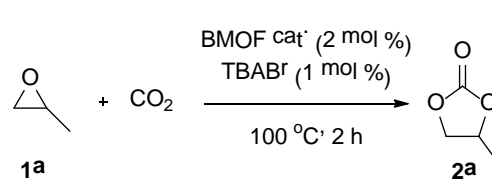
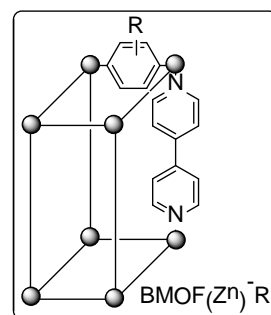


Figure 4. PXRD patterns of BMOFs (BPY MOFs) with different functionalities on the BDC ligand.

From the study with BMOF(Zn)s evaluating the effects of the functional group, all five-functionalized BMOF(Zn)s displayed very similar catalytic activities for CO₂ cycloaddition (from 75% to 80%, Table 3). We assumed that in the BMOF(Zn) system, the Lewis acidity of zinc ions in the SBU and BPY had a more significant effect than the BDC ligand part on the CO₂ cycloaddition. Since the ligand accessibility and synthetic efficiency of BMOF(Zn)-NH₂ is much higher than those of the other BMOF(Zn)s, next, the substrate scopes were investigated with the BMOF(Zn)-NH₂ catalyst (Scheme 1). Alkyl chain-containing butylene oxide and hexylene oxide (i.e., 1,2-epoxybutane (**1b**) and 1,2-epoxyhexane (**1c**)) along with heteroatom-containing (i.e., O and Cl) 1,2-ethoxy-3-methoxypropane (**1d**) and epichlorohydrin (**1e**) were successfully coupled with CO₂ to the corresponding cyclic carbonates with good to excellent yields (71–84%) under the optimized conditions. In case of the simple PO (**1a**) case, 78% yield under 100 °C for 2 h is generally competitive than other MOF conditions with relatively short reaction time (<2 h). Lewis acidic zirconium-based UiO-66 showed 66% under 100 °C for 2 h with PO (**1a**) [14]. Other zinc and BPY-based UMCM-15 is working at room temperature for CO₂ cycloaddition, however longer reaction time (>16 h) is necessary for >90% conversion [25]. In case of cobalt-BPY type MOF, cyclic carbonate synthesis from PO (**1a**) with >90% conversion was obtained under 100 °C for 8 h condition [26]. Next, less reactive di-substituted epoxides were tested for the cycloaddition. 1,2-Epoxy-2-methylpropane (**1f**) and cyclohexene oxide (**1g**) showed relatively low conversion (17% for **2f** and 23% for **2g**, respectively). The obtained products were confirmed by ¹H and ¹³C NMR (see the supplementary information for details), and once again, the polymerized byproduct was not detected in all substrates.

Table 3. Functional group controls in BMOF(Zn)s.



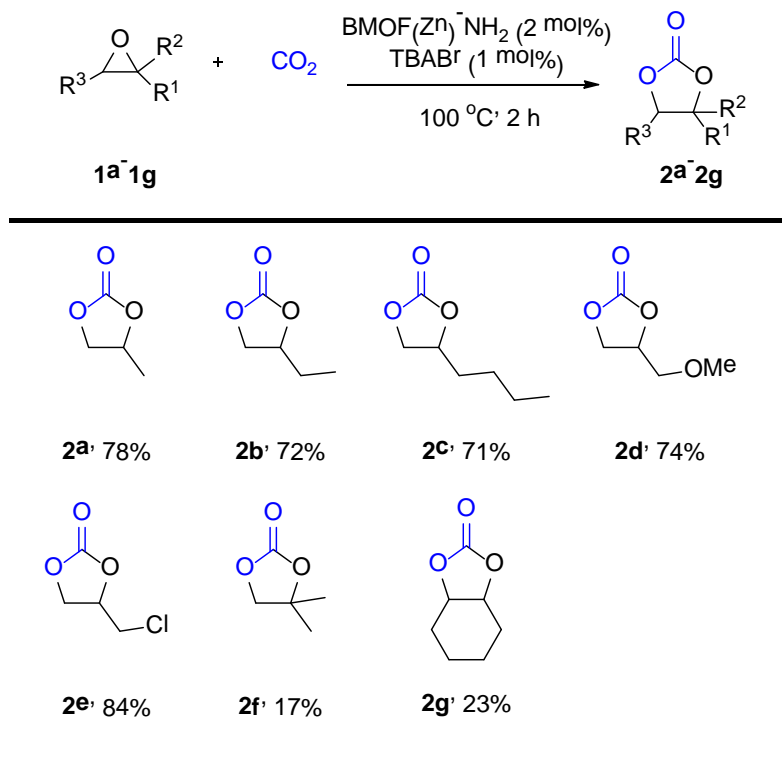


Entry	MOF Catalyst	Conversion (%)	Selectivity (%)
1	BMOF(Zn)	78	>99
2	BMOF(Zn)-NH ₂	78	>99
3	BMOF(Zn)-OH	79	>99
4	BMOF(Zn)-1,4-NDC	80	>99
5	BMOF(Zn)-2,6-NDC	75	>99

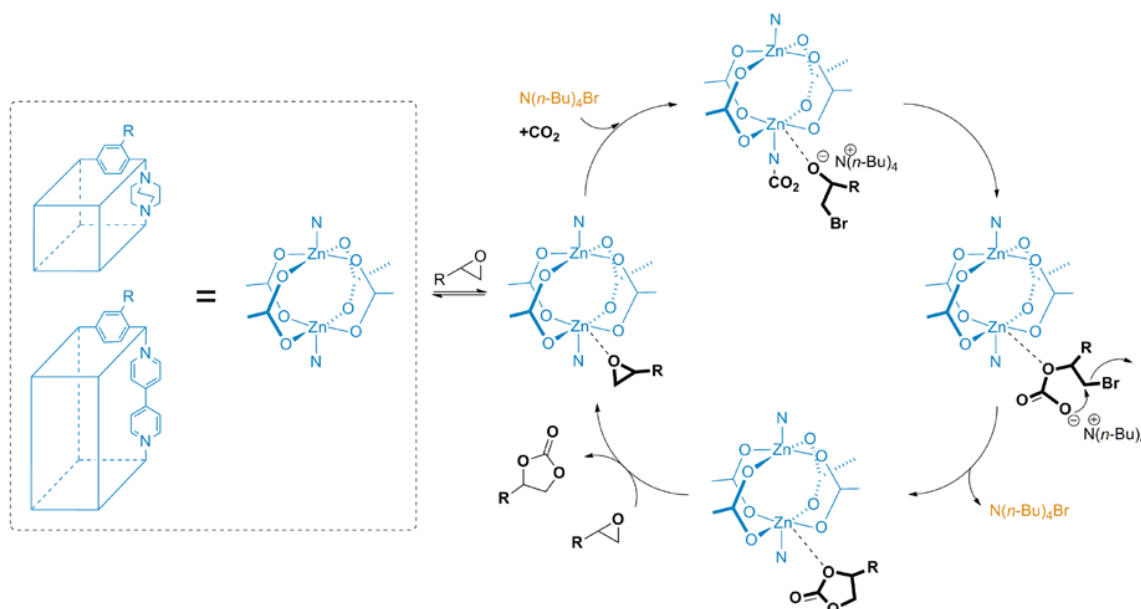
Lastly, the reusability test was performed using the BMOF(Zn)-NH₂ catalyst at 100 °C for 2 h with **1a**. After each cycloaddition reaction, the BMOF(Zn)-NH₂ catalyst was recovered by centrifugation and filtered as a powder, since the crystal was ground by the stir-bar in the reaction vessel. The obtained powder form of BMOF(Zn)-NH₂ after the first and third cycles also showed similar PXRD patterns with the pristine material (Figure S16). And the reactivity of BMOF(Zn)-NH₂ was generally retained by reuse, with values of 75%, respectively (Table S4). This is a somewhat surprising finding because the physical and chemical stabilities of Zn-based pillared MOFs are relatively lower than early transition metal-based MOFs, such as Zr-based MOFs [14,27,28].

A possible reaction mechanism for pillared MOF-catalyzed CO₂ cycloaddition was proposed in the Scheme 2 based on our findings and related references [25,26]. The halide (e.g., bromide) nucleophile from ammonium salt is a key component for the ring-opening of epoxide, and Lewis acidic site on metal SBU could activate the ring-opening of epoxide [14]. The basic site on pillar ligand

will coordinate and activate CO₂ molecule [25,26]. These types of synergic effects between the Lewis acidic sites on metal clusters and basic sites on ligand were previously studied for the cycloaddition reaction in heterogeneous catalysis and ionic liquid [29–31].



Scheme 1. Various organic cyclic carbonates synthesized by BMOF(Zn)-NH₂.



Scheme 2. Proposed reaction mechanism for CO₂ cycloaddition-catalyzed by pillared MOFs.

3. Materials and Methods

Unless otherwise mentioned, all reagents were purchased from chemical companies and vendors and used as received without further purification. DABCO was purified through sublimation before

MOF synthesis. Nickel(II) nitrate hexahydrate (99.999%), cobalt(II) nitrate hexahydrate, copper(II) nitrate trihydrate, terephthalic acid, DABCO (98%), and copper sulfate (98%) were purchased from Sigma-Aldrich (St. Louis, MO, USA). 4,4'-bipyridyl and naphthalene-2,6-dicarboxylic acid were obtained from TCI (Tokyo, Japan). Zinc nitrate hexahydrate (99%), 2-aminoterephthalic acid (99%), naphthalene-1,4-dicarboxylic acid (>98%), and sodium nitrite (98%) were purchased from Alfa-Aesar (Thermo Fischer, Waltham, MA, USA). Chloroform (99.5%), *N,N*-dimethylformamide (DMF, 99.0%), ethyl alcohol (94.5%), hydrochloric acid (35~37%), and sodium hydroxide (beads, 98.0%) were purchased from Samchun (Seoul, Korea). Carbon dioxide gas (99.999%) was consumed for the catalytic reaction.

3.1. Synthesis of 2-Hydroxy Benzene-1,4-Dicarboxylic acid (BDC-OH)

BDC-OH was synthesized by following a reported procedure [32]. The hydroxy group was introduced into 2-amino benzene-1,4-dicarboxylic acid (BDC-NH₂) through the Sandmeyer reaction.

3.2. Synthesis of DMOF(M)s (M: Zn, Cu, Co, Ni)

DMOF(M) was prepared by following a reported method with some modifications (see the supplementary file for details). Metal nitrate (0.20 mmol), BDC ligand (0.20 mmol), DABCO (0.32 mmol) and DMF (4 mL) were placed in a flask. After stirring for 10 min, a white gel was formed. This gel was filtered using a fine porosity glass filter. The clear solution was then transferred to a 20 mL size scintillation vial and heated at 120 °C for 48 h. The resulting crystals were then washed three times with 5 mL of DMF. The solvent was then exchanged with CHCl₃ (3 times), and CHCl₃ was replaced with fresh CHCl₃ every 24 h (3 times).

3.3. Synthesis of Functionalized DMOFs

DMOF(Zn)-R was prepared by following a reported procedure with the target ligand, but with slight modifications (see the supplementary file for details) [33]. Zn(NO₃)₂·6H₂O (59 mg, 0.20 mmol), BDC-R ligand (0.20 mmol), DABCO (36 mg, 0.32 mmol) and DMF (5 mL) were placed in a flask. After stirring for 10 min, the gel was formed. This gel was filtered, and the clear solution was transferred to a 20 mL scintillation vial and heated to 100 °C at a rate of 2.5 °C/min. The temperature was then held for 12 h (at 100 °C), followed by cooling to room temperature at a rate of 2.5 °C/min. The resulting crystals were washed three times with 5 mL of DMF, and the solvent was exchanged with CHCl₃ (3 times), with the CHCl₃ replaced every 24 h (3 times).

3.4. Synthesis of Functionalized BMOFs

BMOF(Zn)-R was synthesized by following a previously reported procedure with slight modifications (see the supplementary file for details) [23,24]. Zn(NO₃)₂·6H₂O (71 mg, 0.24 mmol), BDC-R ligand (0.24 mmol) and BPY (18 mg, 0.12 mmol) were dissolved in DMF/EtOH (1:1, 20 mL) solution. The mixture was stirred for 10 min, transferred to 50 mL size Teflon-lined autoclave and heated at 90 °C for 24 h. The resulting crystals were washed with DMF (5 mL, 3 times), the solvent was exchanged with CHCl₃ (3 times), and CHCl₃ was replaced every 24 h (3 times).

4. Conclusions

The three-component controls in pillared MOFs have been studied for the catalytic CO₂ cycloaddition reaction. Among the various divalent metal sources, Zn(II) displayed the best activity with the existence of ammonium halide co-catalyst at 100 °C. In the case of DABCO-type pillared MOFs, for the DMOF series, the hydroxy group-containing DMOF(Zn)-OH showed the best catalytic activity for CO₂ cycloaddition with PO. For the longer BPY-type pillared MOFs, the functional group in the BDC ligand did not have a significant effect on the CO₂ cycloaddition. Various epoxides were successfully converted to organic cyclic carbonates under the optimized conditions (yields of 71–84%),

and finally pillared MOF, BMOF(Zn)-NH₂ could be recycled up to three times without activity and crystallinity loss.

Supplementary Materials: The following are available online at <http://www.mdpi.com/2073-4344/8/11/565/s1>, Figure S1: ¹H NMR of DMOF(Zn) after acid digestion, Figure S2: ¹H NMR of DMOF(Zn)-NH₂ after acid digestion, Figure S3: ¹H NMR of DMOF(Zn)-OH after acid digestion, Figure S4: ¹H NMR of DMOF(Zn)-1,4-NDC after acid digestion, Figure S5: ¹H NMR of DMOF(Zn)-1,5-NDC after acid digestion, Figure S6: Crystal images of functionalized DMOFs, Figure S7: ¹H NMR of BMOF(Zn) after acid digestion, Figure S8: ¹H NMR of BMOF(Zn)-NH₂ after acid digestion, Figure S9: ¹H NMR of BMOF(Zn)-OH after acid digestion, Figure S10: ¹H NMR of BMOF(Zn)-1,4-NDC after acid digestion, Figure S11: ¹H NMR of BMOF(Zn)-2,6-NDC after acid digestion, Figure S12: SEM image of functionalized BMOF(Zn)s, Figure S13: Structure of BMOF(Zn)-OH (a) top view (b) SBU-focused structure, Figure S14: N₂ full isotherm (77 K) for BMOF(Zn)-OH, Figure S15: Thermogravimetric analysis of BMOF(Zn)-OH, Figure S16: PXRD patterns of BMOF(Zn)-NH₂ before and after reaction, Table S1: Crystallographic data and parameters for BMOF(Zn)-OH, Table S2: Selected bond lengths (Å) and angles (deg) for BMOF(Zn)-OH, Table S3: Reported BET value of DMOF and BMOF series, Table S4: Recycle test results from BMOF(Zn)-NH₂ catalyzed CO₂ cycloaddition with PO, Appendix I: ¹H and ¹³C NMR of the obtained compounds.

Author Contributions: Conceptualization, M.H.P., Y.K. and M.K.; Investigation, J.N., D.K., J.L. and M.Y.; Characterization, J.N. and K.M.L.; Writing-Original Draft Preparation, J.N. and M.K.; Supervision, K.M.L., Y.K. and M.K.

Funding: This work was supported by the Korea Institute of Energy Technology Evaluation and Planning (KETEP) and the Ministry of Trade, Industry and Energy (MOTIE) of the Republic of Korea (No. 20172010202000).

Acknowledgments: We thank Dongwook Kim (IBS) for assistance with X-ray crystallography.

Conflicts of Interest: The authors declare no conflict of interest.

References

1. Kaskel, S. *The Chemistry of Metal-Organic Frameworks, 2 Volume Set: Synthesis, Characterization, and Applications*; Wiley-VCH: Weinheim, Germany, 2016; ISBN 3527338748.
2. MacGillivray, L.R. *Metal-Organic Frameworks: Design and Application*; John Wiley & Sons: Hoboken, NJ, USA, 2010; ISBN 0470195568.
3. Sumida, K.; Rogow, D.L.; Mason, J.A.; McDonald, T.M.; Bloch, E.D.; Herm, Z.R.; Bae, T.-H.; Long, J.R. Carbon Dioxide Capture in Metal-Organic Frameworks. *Chem. Rev.* **2012**, *112*, 724–781. [[CrossRef](#)] [[PubMed](#)]
4. Li, J.-R.; Sculley, J.; Zhou, H.-C. Metal-Organic Frameworks for Separations. *Chem. Rev.* **2012**, *112*, 869–932. [[CrossRef](#)] [[PubMed](#)]
5. Horcajada, P.; Gref, R.; Baati, T.; Allan, P.K.; Maurin, G.; Couvreur, P.; Férey, G.; Morris, R.E.; Serre, C. Metal-Organic Frameworks in Biomedicine. *Chem. Rev.* **2012**, *112*, 1232–1268. [[CrossRef](#)] [[PubMed](#)]
6. Lee, J.; Farha, O.K.; Roberts, J.; Scheidt, K.A.; Nguyen, S.T.; Hupp, J.T. Metal-organic framework materials as catalysts. *Chem. Soc. Rev.* **2009**, *38*, 1450–1459. [[CrossRef](#)] [[PubMed](#)]
7. Yoon, M.; Srirambalaji, R.; Kim, K. Homochiral Metal-Organic Frameworks for Asymmetric Heterogeneous Catalysis. *Chem. Rev.* **2012**, *112*, 1196–1231. [[CrossRef](#)] [[PubMed](#)]
8. Zhu, L.; Liu, X.-Q.; Jiang, H.-L.; Sun, L.-B. Metal-Organic Frameworks for Heterogeneous Basic Catalysis. *Chem. Rev.* **2017**, *117*, 8129–8176. [[CrossRef](#)] [[PubMed](#)]
9. Schejn, A.; Aboulaich, A.; Balan, L.; Falk, V.; Lalevé, J.; Medjahdi, G.; Aranda, L.; Mozet, K.; Schneider, R. Cu²⁺-doped zeolitic imidazolate frameworks (ZIF-8): Efficient and stable catalysts for cycloadditions and condensation reactions. *Catal. Sci. Technol.* **2015**, *5*, 1829–1839. [[CrossRef](#)]
10. Babu, R.; Roshan, R.; Kathalikkattil, A.C.; Kim, D.W.; Park, D.-W. Rapid, Microwave-Assisted Synthesis of Cubic, Three-Dimensional, Highly Porous MOF-205 for Room Temperature CO₂ Fixation via Cyclic Carbonate Synthesis. *ACS Appl. Mater. Interfaces* **2016**, *8*, 33723–33731. [[CrossRef](#)] [[PubMed](#)]

11. Beyzavi, M.H.; Stephenson, C.J.; Liu, Y.; Karagiari, O.; Hupp, J.T.; Farha, O.K. Metal-Organic Framework-Based Catalysts: Chemical Fixation of CO₂ with Epoxides Leading to Cyclic Organic Carbonates. *Front. Energy Res.* **2015**, *2*, 63. [[CrossRef](#)]
12. He, H.; Perman, J.A.; Zhu, G.; Ma, S. Metal-Organic Frameworks for CO₂ Chemical Transformations. *Small* **2016**, *12*, 6309–6324. [[CrossRef](#)] [[PubMed](#)]
13. Adhikari, D.; Nguyen, S.T.; Baik, M.-H. A computational study of the mechanism of the [(salen)Cr⁺ DMAP]-catalyzed formation of cyclic carbonates from CO₂ and epoxide. *Chem. Commun.* **2014**, *50*, 2676–2678. [[CrossRef](#)] [[PubMed](#)]
14. Noh, J.; Kim, Y.; Park, H.; Lee, J.; Yoon, M.; Park, M.H.; Kim, Y.; Kim, M. Functional group effects on a metal-organic framework catalyst for CO₂ cycloaddition. *J. Ind. Eng. Chem.* **2018**, *64*, 478–483. [[CrossRef](#)]
15. Chun, H.; Dybtsev, D.N.; Kim, H.; Kim, K. Synthesis, X-ray crystal structures, and gas sorption properties of pillared square grid nets based on paddle-wheel motifs: Implications for hydrogen storage in porous materials. *Chem. Eur. J.* **2005**, *11*, 3521–3529. [[CrossRef](#)] [[PubMed](#)]
16. Dybtsev, D.N.; Chun, H.; Kim, K. Rigid and Flexible: A Highly Porous Metal–Organic Framework with Unusual Guest-Dependent Dynamic Behavior. *Angew. Chem. Int. Ed.* **2004**, *43*, 5033–5036. [[CrossRef](#)] [[PubMed](#)]
17. Kim, H.-J.; Kurisingal, J.F.; Park, D.-W. Ni₂(BDC)₂(DABCO) metal–organic framework for cyclic carbonate synthesis from CO₂ and epoxides (BDC = 1,4-benzendicarboxylic acid, DABCO = 1,4-diazabicyclo[2.2.2]octane). *React. Kinet. Mech. Catal.* **2018**, *124*, 335–346. [[CrossRef](#)]
18. Cho, W.; Shin, M.S.; Hwang, S.; Kim, H.; Kim, M.; Kim, J.G.; Kim, Y. Tertiary amines: A new class of highly efficient organocatalysts for CO₂ fixations. *J. Ind. Eng. Chem.* **2016**, *44*, 210–215. [[CrossRef](#)]
19. Mousavi, B.; Chaemchuen, S.; Moosavi, B.; Zhou, K.; Yusubov, M.; Verpoort, F. CO₂ Cycloaddition to Epoxides by using M-DABCO Metal-Organic Frameworks and the Influence of the Synthetic Method on Catalytic Reactivity. *ChemistryOpen* **2017**, *6*, 674–680. [[CrossRef](#)] [[PubMed](#)]
20. Kim, M.; Boissonnault, J.A.; Dau, P.V.; Cohen, S.M. Metal-Organic Framework Regioisomers Based on Bifunctional Ligands. *Angew. Chem. Int. Ed.* **2011**, *50*, 12193–12196. [[CrossRef](#)] [[PubMed](#)]
21. Hahm, H.; Yoo, K.; Ha, H.; Kim, M. Aromatic Substituent Effects on the Flexibility of Metal–Organic Frameworks. *Inorg. Chem.* **2016**, *55*, 7576–7581. [[CrossRef](#)] [[PubMed](#)]
22. Ha, H.; Hahm, H.; Jwa, D.G.; Yoo, K.; Park, M.H.; Yoon, M.; Kim, Y.; Kim, M. Flexibility in metal–organic frameworks derived from positional and electronic effects of functional groups. *CrystEngComm* **2017**, *19*, 5361–5368. [[CrossRef](#)]
23. Chen, B.; Liang, C.; Yang, J.; Contreras, D.S.; Clancy, Y.L.; Lobkovsky, E.B.; Yaghi, O.M.; Dai, S. A microporous metal-organic framework for gas-chromatographic separation of alkanes. *Angew. Chem. Int. Ed.* **2006**, *45*, 1390–1393. [[CrossRef](#)] [[PubMed](#)]
24. Jasuja, H.; Walton, K.S. Effect of catenation and basicity of pillared ligands on the water stability of MOFs. *Dalton Trans.* **2013**, *42*, 15421–15426. [[CrossRef](#)] [[PubMed](#)]
25. Babu, R.; Kim, S.H.; Kathalikkattil, A.C.; Kuruppathparambil, R.R.; Kim, D.W.; Cho, S.J.; Park, D.W. Aqueous microwave-assisted synthesis of non-interpenetrated metal-organic framework for room temperature cycloaddition of CO₂ and epoxides. *Appl. Catal. A Gen.* **2017**, *544*, 126–136. [[CrossRef](#)]
26. Song, X.; Wu, Y.; Pan, D.; Zhang, J.; Xu, S.; Gao, L.; Wei, R.; Zhang, J.; Xiao, G. Dual-linker metal-organic frameworks as efficient carbon dioxide conversion catalysts. *Appl. Catal. A Gen.* **2018**, *566*, 44–51. [[CrossRef](#)]
27. Low, J.J.; Benin, A.I.; Jakubczak, P.; Abrahamian, J.F.; Faheem, S.A.; Willis, R.R. Virtual High Throughput Screening Confirmed Experimentally: Porous Coordination Polymer Hydration. *J. Am. Chem. Soc.* **2009**, *131*, 15834–15842. [[CrossRef](#)] [[PubMed](#)]
28. Burtch, N.C.; Jasuja, H.; Walton, K.S. Water Stability and Adsorption in Metal–Organic Frameworks. *Chem. Rev.* **2014**, *114*, 10575–10612. [[CrossRef](#)] [[PubMed](#)]
29. Yang, Z.-Z.; He, L.-N.; Miao, C.-X.; Chanfreau, S. Lewis Basic Ionic Liquids-Catalyzed Conversion of Carbon Dioxide to Cyclic Carbonates. *Adv. Synth. Catal.* **2010**, *352*, 2233–2240. [[CrossRef](#)]
30. Adeleye, A.I.; Patel, D.; Niyogi, D.; Saha, B. Efficient and Greener Synthesis of Propylene Carbonate from Carbon Dioxide and Propylene Oxide. *Ind. Eng. Chem. Res.* **2014**, *53*, 18647–18657. [[CrossRef](#)]

31. Tu, M.; Davis, R.J. Cycloaddition of CO₂ to Epoxides over Solid Base Catalysts. *J. Catal.* **2001**, *199*, 85–91. [[CrossRef](#)]
32. Himsl, D.; Wallacher, D.; Hartmann, M. Improving the Hydrogen-Adsorption Properties of a Hydroxy-Modified MIL-53(Al) Structural Analogue by Lithium Doping. *Angew. Chem. Int. Ed.* **2009**, *48*, 4639–4642. [[CrossRef](#)] [[PubMed](#)]
33. Hahm, H.; Ha, H.; Kim, S.; Jung, B.; Park, M.H.; Kim, Y.; Heo, J.; Kim, M. Synthesis of secondary and tertiary amine-containing MOFs: C–N bond cleavage during MOF synthesis. *CrystEngComm* **2015**, *17*, 5644–5650. [[CrossRef](#)]



© 2018 by the authors. Licensee MDPI, Basel, Switzerland. This article is an open access article distributed under the terms and conditions of the Creative Commons Attribution (CC BY) license (<http://creativecommons.org/licenses/by/4.0/>).